eJSE International

Electronic Journal of Structural Engineering 11(1) 2011

Eccentric force excitation of a reinforced concrete building to assess torsion amplification

J. De-la-Colina and J. Valdés
Facultad de Ingeniería, Universidad Autónoma del Estado de México, Toluca, México.
Email: *jaime_delacolina@yahoo.com*

ABSTRACT: Dynamic analysis should be preferred for seismic design of buildings and other structures instead of a static one. However, in several current building codes seismic static design of buildings requires an amplification of torsion moments (or story eccentricities) computed from lateral forces statically applied at floor levels. Discrepancy of factors used to estimate torsion amplification among codes suggests further study on this subject. The main objective of this paper is to show estimations of the building dynamic torsion. These estimations were obtained from experiments conducted in a four-story reinforced concrete building without accidental eccentricity that was excited with a dynamic force generator placed at the roof. The exciter was operated at several frequencies and it was placed at two roof positions. By assuming three degrees of freedom for each building slab and using acceleration records from tests, equations of motion of the system were used to estimate dynamic story torsional moments. Results support the idea that building torsional response also depends on coupling between the excitation force frequency and the building modal frequencies associated with torsion (either pure torsion or translation coupled with torsion).

Keywords: Experimental testing; torsion amplification; static design; torsional response.

1 INTRODUCTION

Dynamic analysis should be preferred for seismic design of buildings and other structures instead of a static one. However, current building codes (ICC 2006, DDF 2004, ACNBC 2005) and some recommendations (BSSC 2003) still allow static analyses/designs. In the case of torsionally unbalanced buildings, static design usually allows to incorporate the effect of both slab rotational inertia and damping through the use of an amplification factor (usually identified as α or A_x) to estimate the lateral effects that a dynamic analysis would provide. The commonly used equations (De la Llera & Chopra 1994) to refer to this factor are expressed in terms of two design eccentricities e_d:

$$e_{d1} = \alpha e_s + \beta b = \alpha e_s + e_a \quad (1a)$$

$$e_{d2} = \delta e_s - \beta b = \delta e_s - e_a \quad (1b)$$

where α is the amplification factor that increases the story (natural or inherent) eccentricity e_s and δ is a factor to reduce e_s. The factor β is used to estimate the accidental eccentricity e_a in terms of the building plan dimension normal to the direction of the ground motion, b. These eccentricities are combined with the (static) story shear forces (V) to obtain approximations to the story torsion moments that could be obtained from a dynamic analysis (M_{dyn}). Notice in these traditional equations that amplification only applies to the natural eccentricity, although there is no reason to discard amplification of the accidental one. After all, both eccentricities (e_s and e_a) give place to a total eccentricity. Shear forces and the estimated amplified torsion moments (M_d) are combined at each story to estimate forces at the lateral resisting elements. Notice that in general $M_d \neq M_{dyn}$. For design of a given structural element, the selection of a design eccentricity (either e_{d1} or e_{d2}) is based on the combination of V and M_d that causes the largest element lateral force.

It is interesting to observe that, as for the factor α is concerned, some building codes specify different values (ICC 2006, DDF 2004, ACNBC 2005), as follows: IBC (2006): $\alpha = 1.0$; MCBC (2004): $\alpha = 1.5$; NBCC (2005): $\alpha = 1.5$. There is also a significant difference between the ASCE 7-05 standard (ASCE 2005) and the NEHRP provisions (BSSC 2003). While in the ASCE-7-05 and IBC (2006) standards the amplification factor A_x applies only to the accidental eccentricity e_a, in the 2003 NEHRP provisions the amplification factor A_x applies to the sum of e_s and e_a. In both cases, the same formula to compute the design amplification factor (A_x) is used,

which is defined as follows, with $1.0 \leq A_x \leq 3.0$:

$$A_x = \left(\frac{\delta_{max}}{1.2\delta_{avg}}\right)^2 \quad (2)$$

where δ_{max} is the maximum displacement at the story while δ_{avg} is the average displacement of the extreme points of the same structural level.

Two interesting points of this formula to estimate torsion amplification are pinpointed. First, when this expression is used amplification increases with eccentricity magnitude. This is different to the traditional recommendation of using a single value of α for all values of eccentricity. This increment with eccentricity implicit in Equation 2 is not consistent with other previous results (Chandler & Hutchinson 1988, Chandler & Duan 1993, De-la-Colina 2003, De-la-Colina et al. 2007) that indicate amplification reductions with eccentricity in order to achieve uniform values of ductility demands. Second, the amplification magnitude given by Equation 2 can result in factors up to twice larger than those obtained with traditional formulas.

The previous differences of the referred building codes and recommendations clearly indicate that the static torsion design procedure for buildings should be restated. However, regardless of both the variation of the amplification factor or the magnitude of the accidental eccentricity, the (total) eccentricity of a building story is unique and, therefore, the dynamic amplification should apply to both static estimates e_s and e_a, as explained below.

Two alternative ways within a static design can be identified: If e_a is a static estimate of the accidental eccentricity, then the amplification factor should apply to both eccentricities (e_s and e_a) as indicated before (consistent in this respect with the 2003 NEHRP provisions (BSSC 2003)). On the other hand, if e_a was a dynamic estimate of the accidental eccentricity, then the amplification factor should apply to the natural eccentricity (e_s) only, as implied by the traditional Equations 1.

In case of a dynamic analysis the previous analysis has a parallel rationale when e_a is included within a structural model: If e_a is a static estimate of the accidental eccentricity, then a dynamic analysis will amplify both eccentricities (e_s and e_a). On the other hand, if e_a were a dynamic estimate of the accidental eccentricity, then a dynamic analysis will amplify once the natural eccentricity and twice the accidental eccentricity.

Last two paragraphs indicate that the assumption that e_a is a static estimate is more reasonable than assuming that e_a is a dynamic estimate. Therefore the amplification factor (called either α or A_x) should amplify both e_s and e_a.

It is the opinion of the authors that an additional study of α (or A_x) is required, preferably consistent with experimental results. A number of studies have been carried out before to assess values of factor α. However, most of them have been analytical (Duan & Chandler 1993). Experimentally, few studies have been also performed to assess α. For instance, De-la-Colina et al. (2007) used a simple two-story moment resistant frame without accidental eccentricity to estimate α. They reported values of α close to 2.0 for small-eccentricity models. In actual buildings, the estimation of this factor is not simple because it is difficult to identify the contribution of the accidental eccentricity from the total response. It is well known that in buildings, partitions, ceilings, stairs, and live load, among others, lead to building accidental rotations which are difficult to evaluate.

A first step toward the assessment of torsion amplification factors is the computation of story dynamic torsional moments. These dynamic moments also permit to obtain a better understanding of the structure torsion behavior during earthquakes.

The main objective of this paper is to show assessments of the building dynamic torsion obtained from forced-vibration studies carried out in a four-story reinforced-concrete building with practically no accidental eccentricity. This condition ($e_a \approx 0$) was achieved by testing the building just before installation of nonstructural elements and application of live load. The good quality of materials and construction procedures also contributed to attain almost-zero accidental eccentricity. This condition is analyzed in the next sections. Because the building had one symmetry axis, the eccentricity was only due to the location of the exciter for loads parallel to the symmetry axis. The low level of structural damping, which was also due to the lack of nonstructural elements, also simplified the estimation of the dynamic torsions. Building tests were carried out within the building elastic behavior.

2 THE BUILDING

A four-story reinforced concrete building, planned for government offices, was tested. It is located on firm soil in the city of Toluca, Mexico. The structure consists of orthogonal frames separated 6.00 m in both directions. The reinforced concrete columns and beams are rectangular with dimensions of 40 x 55 cm and 30 x 60 cm, respectively. Waffle slabs with thickness equal to 30 cm are supported on beams. Figure 1 shows the geometry of the building structural frames. A particular characteristic of the building is its irregularity in the longitudinal direction (E-W) caused by the set-backs of upper stories;

however, in the transversal direction (N-S) the structure is regular. The irregular condition is due to the lack of vertical alignment of the centers of mass of each floor. Therefore, the structure is susceptible to torsion response to base excitation in the north-south direction.

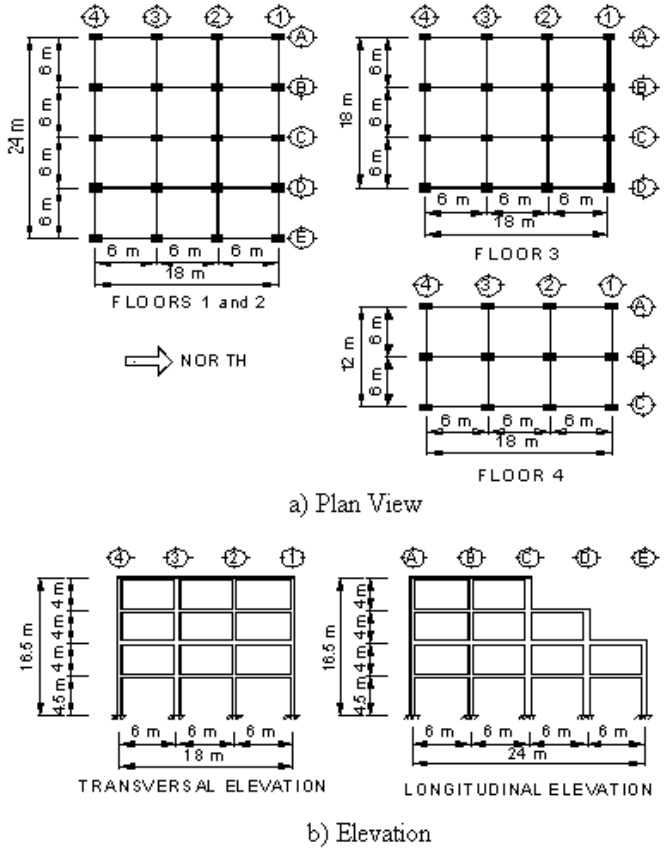

Figure 1. Geometry of the tested building

The tested structure forms part of a bigger construction complex, so the referred structure is only one of the bodies of the whole building. Figure 2a shows a front-view image of the tested building. Figure 2b shows the lateral view of the building.

An important condition of the building during testing was that the structure did not have non-structural elements such as separation walls, windows, doors, ceilings, installations, etc. Moreover, the structure had neither stairs nor slab openings. Tests were conducted after the building structure construction finished, but before non-structural elements were attached.

In accordance with design specifications, concrete with $f'_c = 25$ MPA (250 kg/cm^2) and reinforcing steel with $f_y = 420$ MPA (4,200 kg/cm^2) were used. The foundation of the building is a 30 cm -thick reinforced concrete slab with 80 cm -depth beams. Reinforced concrete weight resulted equal to 22,650 N/m^3, approximately.

Building modal frequencies were obtained using several frequency domain identification techniques such as the mean value of the normalized singular values of the density spectral matrices, the coherence between couples of acceleration records and the Fourier´s amplitude of response records. The results obtained with these identification techniques are consistent among them for the analyzed cases (De-la-Colina & Valdés 2006, De-la-Colina & Valdés 2007). The acceleration records used for identification of dynamic properties were obtained from several free and forced vibration E-W direction tests conducted on the building.

Figure 2. Condition of the building during testing.

To compare identification experimental results with those obtained with an analytical methodology, a tridimensional finite-element model of the building was developed. Its properties (geometry, materials, etc.) were those of the building nominal design

drawings and specifications, but without live load and using a reduced dead load. The analytical model was calibrated by adjusting the first mode frequency identified from the experimental data with the first mode frequency of the model. This was achieved by increasing 18% the concrete nominal elasticity. Figure 3 shows the mode shapes and frequencies obtained with the finite element model. Table 1 shows a comparison between the building frequencies obtained with the analytical model and those obtained with experimental data. Using the free-vibration decay method a viscous damping ratio $\xi = 0.01$ was obtained.

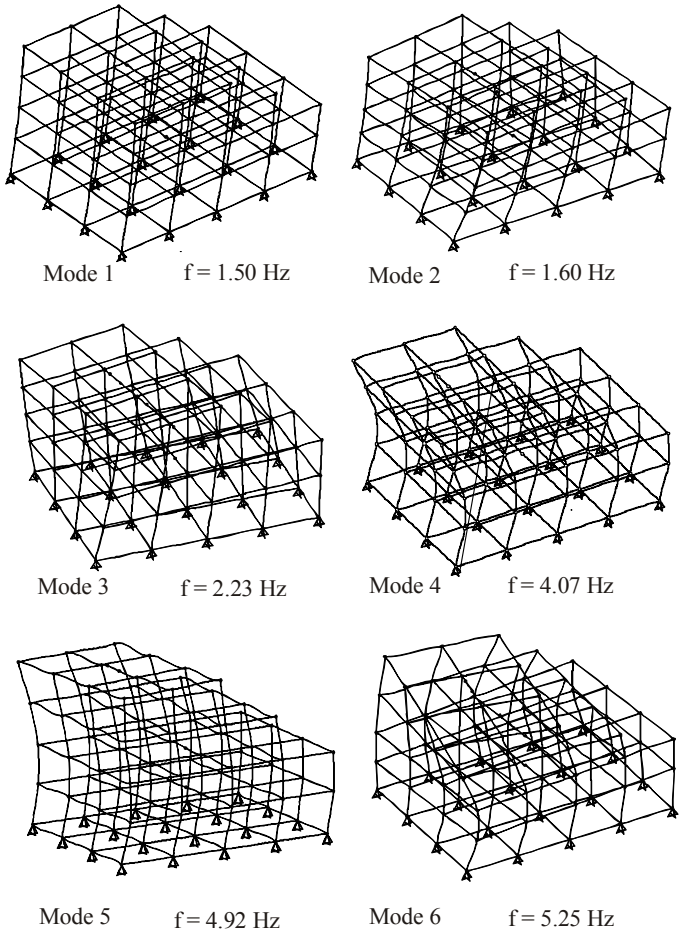

Figure 3. Building analytical mode shapes and frequencies.

3 TESTS

The structure was dynamically excited with a mechanical force generator (shaker or exciter). This device works with two equal eccentric weights rotating in opposite directions to generate a unidirectional harmonic force with magnitude P given by

$$P = 2\,m_1\,r_1\,\bar{\omega}^2 \sin(\bar{\omega}t)$$

$$P = 2(W_1\,r_1/g)\,\bar{\omega}^2 \sin(\bar{\omega}t)$$

$$P = (Wr/g)\bar{\omega}^2 \sin(\bar{\omega}t) \qquad (3)$$

where m_1 is the mass of each rotating weight W_1, r_1 is the mass eccentricity, $\bar{\omega}$ is the rotation frequency of m_1, g is the gravity acceleration, and t denotes time. In the actual exciter, Wr accounts for all rotating weights (baskets, plates, bolts, etc.) that contribute to P.

Table 1. Experimental and analytical mode frequencies.

Mode	Experimental freq. (Hz)	Analytical freq. (Hz)	Difference (%)	Observation
1	1.50	1.50	0.00	Translation (1st mode, E-W)
2	1.75	1.60	9.37	Translation (1st mode, N-S)
3	2.25	2.23	0.89	Torsion (1st mode)
4	3.75	4.07	-7.86	Translation (2nd mode, E-W)
5	Not found	4.92	-	Translation (2nd mode, N-S)
6	5.00	5.25	4.76	Torsion (2nd mode)

The exciter was placed at two different positions on the roof building (indicated with shaded area in Figure 4). Position A corresponded to the geometrical center of the roof, while position B was 2 m eccentric. This exciter eccentric position leads to a ratio $e_{exc}/b \approx 0.10$, with b = the building dimension perpendicular to the direction of the force resultant. Although different excitation directions were considered, in this paper tests associated to the force P acting along the east-west direction are analyzed only.

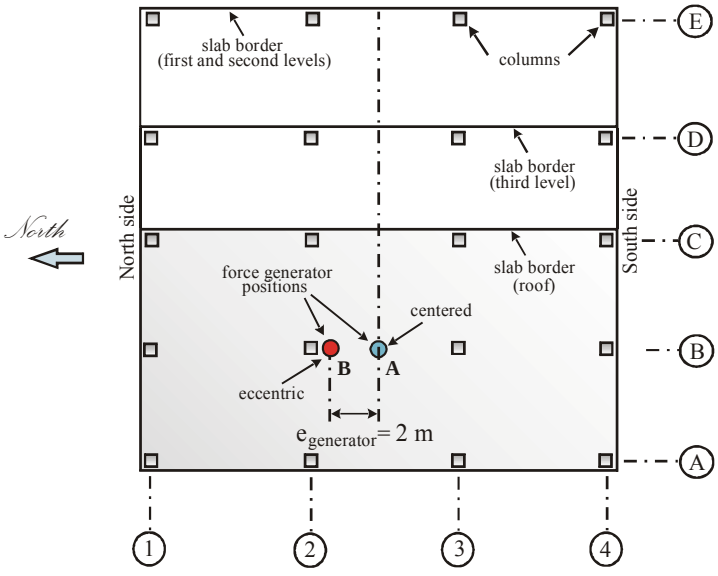

Figure 4. Building plan view showing the exciter positions

For each exciter position, the load P was applied with six different frequencies ($\Omega = \bar{\omega}/2\pi$ = 1.5, 3.0,

3.5, 4.0, 4.5 and 5.0 Hz). In all cases, $2m_1r_1 = 2(W_1 r_1/g) = Wr/g = 23.02$ N·s^2 (2.347 kg.s^2) in Equation 3. Excitation frequencies were selected as follows. After the exciter was installed at the building, an initial exploration of excitation frequencies was carried out to look for those frequencies with large building response. The first modal frequency was clearly identified (close to 1.5 Hz). The following modal frequencies were identified between 3.5 and 5.0 Hz, approximately. By then, the building response was not discriminated either as translational or torsional. For this reason, excitation frequencies were set at intervals of 0.5 Hz from 3.0 to 5.0 Hz, in addition to the first one. Subsequent analytical results and a detailed analysis of the experimental signals showed that the first torsional frequency was close to 2.3 Hz, out of the testing frequency range. Unfortunately, additional tests could not be carried out for the missing frequency range (between 1.5 and 3.0 Hz).

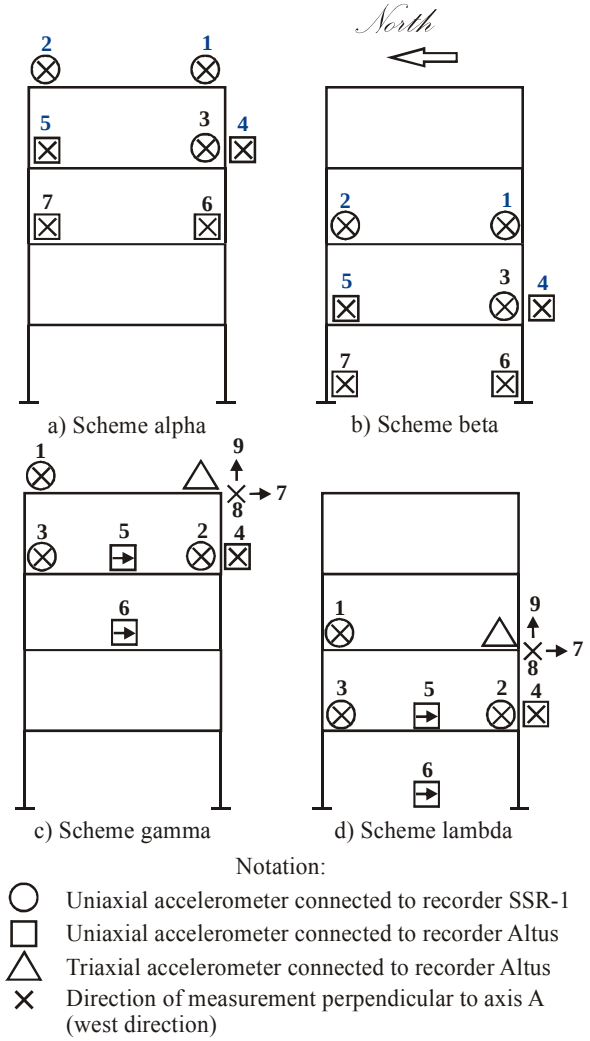

Figure 5. Schemes of locations for accelerometers

The response of the structure was recorded by 7 Kinemetrics® unidirectional accelerometers (4 EpiSensor® FBA-ES-U2 and 3 FBA-11) and one triaxial accelerometer connected to two Kinemetrics® digital recorders (Altus/K2 and SSR-1). All accelerometers were placed along the axis A (building west facade). Four schemes of instrumentation were used for each test associated to a particular frequency, excitation direction, and exciter position. For each test and for each building level, the translation acceleration along the building axes 1 and 4 shown in Figure 5 (east-west direction) and the translation acceleration along the building axis A (north-south direction) were recorded.

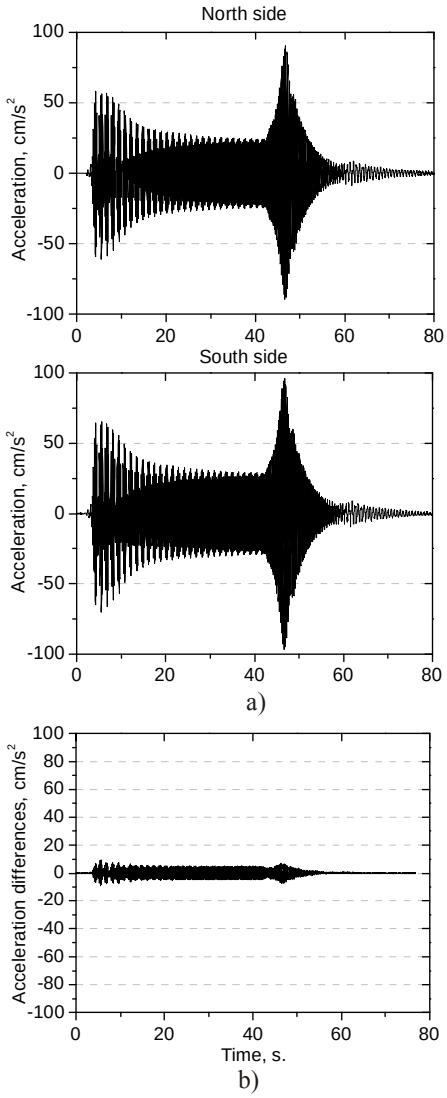

Figure 6. Recorded response for the building 4th level in E-W direction, associated to exciter position A (concentric) and Ω = 4.5 Hz. (a) Accelerations. (b) Acceleration differences.

For the procedure outlined in the methodology section, it is important to analyze the building accidental eccentricity during tests. An east-west excitation with the force generator at position A did not induce structure torsional response, while at position B it did. This showed that torsional response was caused almost exclusively by eccentricity of the applied force, showing that the building practically did

not have accidental eccentricity during tests.

Figure 6 shows the 4th level recorded accelerations for a test with the exciter at position A (not eccentric) and Ω = 4.5 Hz. It is observed that the north side recorded acceleration was similar to that recorded in the south side. On the other hand, Figure 7 shows the same that Figure 6 but with the exciter located at position B (eccentric). Both recorded acceleration (north and south sides) are quite different each other in Figure 7. The small accelerations recorded in the south side in Figure 7 (as compared with those in Figure 6) suggest that for the exciter in eccentric position the slab movement shifts from a translation-dominant movement (Figure 6) to a rotation-dominant movement (Figure 7) with center of rotation close to the building south side.

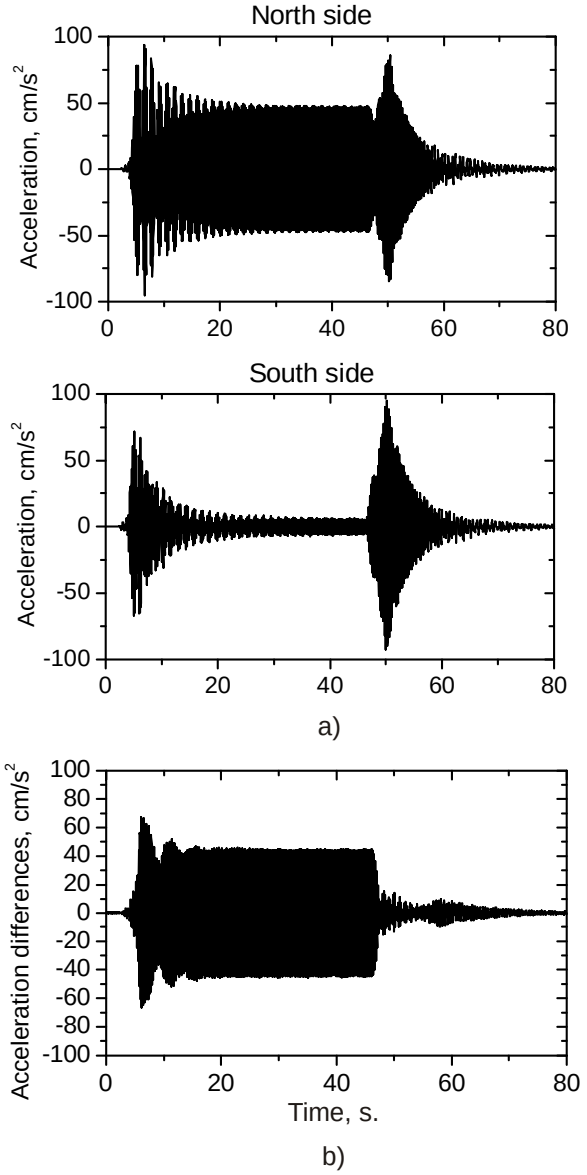

Figure 7. Recorded response for the building 4th level in E-W direction, associated to exciter position B (2 m eccentric) and Ω = 4.5 Hz.(a) Accelerations. (b) Acceleration differences

To analyze the twist of the slabs, the differences of these recorded accelerations (Figures 6a and 7a) were computed. Differences can be seen as an indicator of slab twists. By comparing Figures 6b and 7b, it is clear that the differences between the accelerations recorded in both building sides are much more notable for exciter at position B (Figure 7b) than for exciter at position A (Figure 6b). This corroborates that the most important eccentricity in the building for the excitation along the E-W direction is due to the exciter position. Accidental eccentricity resulted to be so small that it could be neglected.

Differences between E-W accelerations of axes 1 and 4 (Figure 4) were computed to approximate slab acceleration rotations (without dividing by the distance between these two axes). These differences were used also to analyze the effect of the force frequency Ω on the torsional response of the building. Figure 8 shows floor accelerations differences normalized twice, so that all ordinates at Ω = 1.5 Hz resulted equal to 1.0. The first normalization was with respect to the force magnitude for the frequency Ω = 1.5 Hz. This normalization was done to attain acceleration differences independent of the force magnitude. Notice that the applied force magnitude increases with the square of its frequency (Eq. 3).

The second normalization was with respect to the acceleration difference computed for the value Ω = 1.5 Hz. Therefore, ordinates in Figure 8 show relative values of rotational accelerations, independent of force magnitude in terms of the force frequency for Ω = 1.5 Hz. For instance for the 4th floor, this figure indicates that floor acceleration differences (rotations) for operation frequencies of 4.5 and 5.0 Hz can result several times (2 to 5 times) greater than the those corresponding to smaller frequencies (Ω = 1.5, 3.0, or 3.5 Hz). This corroborates that torsional response depends on the excitation frequency. Although it seems an obvious result, this dependency is not currently taken into account in the static torsion design of buildings.

It is observed that excitation frequency of 1.5 Hz coincides with the building first translation modal frequency while the excitation frequency of 5.0 Hz is close to the building second modal frequency associated to torsion (6th mode in Figure 3). The same figure shows that although there is a frequency ratio close to 1.0 in both cases ($\Omega_1/f_1 \approx 1.0$ for the first mode and $\Omega_6/f_6 \approx 1.0$ for the sixth mode), the torsional acceleration for 5 Hz is 4.5 times larger than that recorded for 1.5 Hz. Thus, it can be corroborated with these experimental measurements that building torsion response depends on coupling between the excitation force frequency and the building mode frequencies associated with torsion (either pure torsion or translation coupled with torsion). However,

no current code provisions takes into account this ratio explicitly for static torsion design.

The small response of the 3rd floor for high frequencies (4.5 and 5.0 Hz) can be explained with an analysis of the building second torsional modal response (6th modal shape in Figure 3). This shape shows that both the first and the second floors rotate in the same sense while the fourth floor rotates in the opposite sense. For this mode, the third floor shows a small rotation that can explain the third-floor small acceleration rotations for these high excitation frequencies.

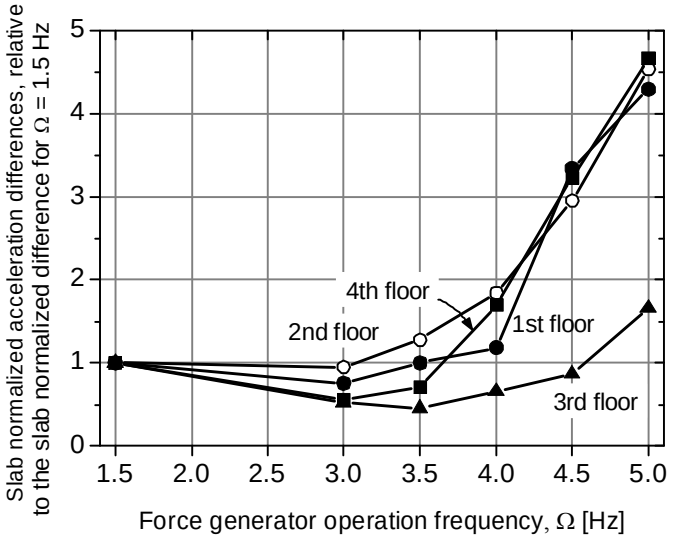

Figure 8. Relative values of floor rotational accelerations, independent of force magnitude

4 METHODOLOGY TO ESTIMATE BUILDING TORSIONAL MOMENTS

One of the objectives of these tests and subject of this paper is to estimate, from building measurements, values of the dynamic torsion. In this section, the procedure to obtain estimations of these torsional moments is described. It can be established that the design torsion moment M_d can be given by the peak dynamic torsion moment $M_{dyn}(t)$, *i.e.*,

$$M_{\mathrm{d}} \approx \max\left\{M_{\mathrm{dyn}}(t)\right\} \tag{4}$$

According to static design procedures, the design torsion moment is given by

$$M_{\mathrm{d}} = F_{\mathrm{st}} \cdot e_{\mathrm{d}} \tag{5}$$

where F_{st} is the static lateral shear force in the story acting at the story shear center (which does not necessarily coincide with center of mass of the corresponding floor). For design, both the torsion moment M_d and the static force F_{st} are superposed to compute the forces (and displacements) of the lateral resisting elements.

To evaluate the dynamic torsion moment for a given building story, the equations of motion of a simplified model of the building are used. In this case, considering three degrees of freedom per floor, the equations of motion can be expressed as follows

$$\mathbf{m}\ddot{\mathbf{u}} + \mathbf{c}\dot{\mathbf{u}} + \mathbf{f} = \mathbf{p} \tag{6}$$

where **m** is the system mass matrix, **c** is the viscous damping matrix, **f** is the restoring force vector, and **p** is the vector of externally applied forces. Here, velocity and acceleration vectors ($\dot{\mathbf{u}}$ and $\ddot{\mathbf{u}}$ respectively) have the arrangement dictated by the displacement vector **u**

$$\mathbf{u}^{\mathrm{T}} = [u_1 \;\; u_2 \;\; u_3 \;\; u_4 \;\; v_1 \;\; v_2 \;\; v_3 \;\; v_4 \;\; \theta_1 \;\; \theta_2 \;\; \theta_3 \;\; \theta_4] \tag{7}$$

while **p** and **f** (which also depend on the time *t*) have the following forms (with $F_{\mathrm{exciter}} = \tilde{F}$)

$$\mathbf{p}^{\mathrm{T}} = [0 \;\; 0 \;\; 0 \;\; \tilde{F} \;\; 0 \;\; 0 \;\; 0 \;\; 0 \;\; 0 \;\; 0 \;\; 0 \;\; \tilde{F} \cdot e_{\mathrm{s}})] \tag{8}$$

$$\mathbf{f}^{\mathrm{T}} = [f_{\mathrm{x1}} \; f_{\mathrm{x2}} \; f_{\mathrm{x3}} \; f_{\mathrm{x4}} \; f_{\mathrm{y1}} \; f_{\mathrm{y2}} \; f_{\mathrm{y3}} \; f_{\mathrm{y4}} \; m_{\mathrm{t1}} \; m_{\mathrm{t2}} \; m_{\mathrm{t3}} \; m_{\mathrm{t4}}] \tag{9}$$

The indexes in vectors **u** and **f** correspond to the floor number as indicated in Figure 9.

From Equation 6, the restoring force **f** can be seen as follows:

$$\mathbf{f} = \mathbf{p} - \mathbf{m}\ddot{\mathbf{u}} - \mathbf{c}\dot{\mathbf{u}} \tag{10}$$

This equation indicates that the restoring force in the structure, which contains both shear forces and torsion moments, can be computed with the force function **p** due to the force generator, the inertia forces, and the damping forces. For the stabilized operation of the generator, which is achieved after a few seconds of starting its electrical motor, the vector **p** is constructed with the following function of the exciter force (see Equation 3)

$$\tilde{F} = (Wr/g)\bar{\omega}^2 \sin(\bar{\omega}t) = A_0 \sin(\bar{\omega}t) \tag{11}$$

where A_0 is the exciter force amplitude. As indicated before, calibration of the exciter allowed to estimate **p** with good accuracy.

Before using Equation 10, floor accelerations were properly scaled, base-line corrected, and bandpass filtered (Ω_{max} = 20 Hz). Moreover, because the mass matrix **m** was a diagonal matrix and **c** was assumed to be proportional to **m** to account mainly for the damping of the first modes (*i.e.*, $\mathbf{c} = a_0\mathbf{m}$), the torsion moments of the restoring forces **f** could be easily computed with the experimentally obtained records A and B indicated in Figure 9. For instance for the top story, the dynamic torsion

moment (12th component of **f**) results:

$$m_{t\,4} = [M_{dyn}]_4 = A_0\, e_s \sin(\bar{\omega}t) - J_4\,(\ddot{u}_{CM})_4 - a_0\, J_4\,(\dot{u}_{CM})_4 \quad (12)$$

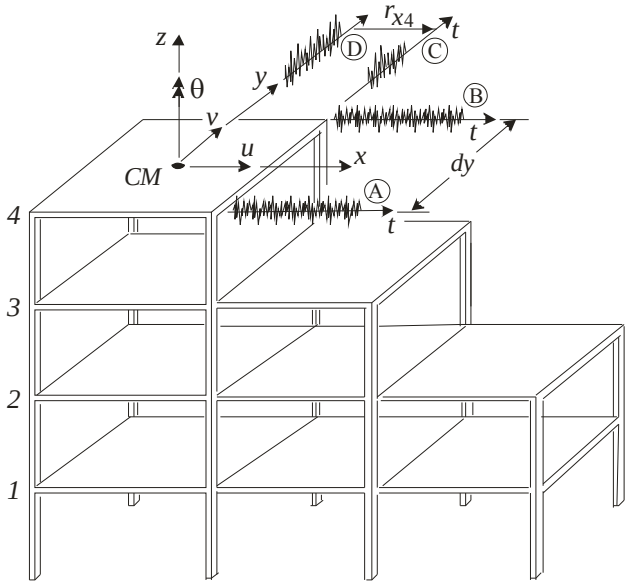

Figure 9. Coordinate system and displacements of a schematic view of the building

where J_4 is the mass moment of inertia of the fourth floor computed with respect to the vertical axis passing through the slab center of mass (in this case the centroid of the slab), $(\ddot{u}_{CM})_4$ is the rotational acceleration of the same floor given by $(\ddot{u}_{CM})_4 = [(\ddot{u}_A)_4 - (\ddot{u}_B)_4]/d_y$, and $(\dot{u}_{CM})_4$ is the corresponding rotational velocity. This rotational velocity was computed by integrating, filtering and base-line correcting the acceleration records. The distance d_y is also indicated in Figure 9.

In this study, the estimated dynamic torsional moment was normalized with respect to the product of the magnitude exciter force (F_{exciter}) and the exciter eccentricity (e_{exc}). The normalization was done in order to show values without units which can be easily compared among them. This normalized dynamic torsional moment can be thought as an amplification factor that increases an applied static torsional moment caused by the exciter, *i.e.*,

$$\alpha^*(t) = M_{dyn}/[F_{\text{exciter}} \cdot e_{exc}] \quad (13)$$

The selected quantities for the normalization were chosen to obtain similar amplification factors to those of building codes. This normalization is used for all stories. The resulting factor α^* is similar to the amplification factor used in static torsion design (Ec. 1a). Although this factor α^* is not the same than the amplification factor used for torsion design in codes, it allows to study the effect of both excitation frequency and eccentricity on the dynamic torsional behavior.

5 RESULTS

As an illustration, values of α^* computed with the procedure previously described are plotted in Figure 10 for a force frequency Ω equal to 3.0 Hz of a short time interval corresponding to the steady-state response. In all cases, the steady-state response was clearly identified for a time interval between 20 and 40 seconds approximately after the excitation started. Each curve in the figure corresponds to a building story.

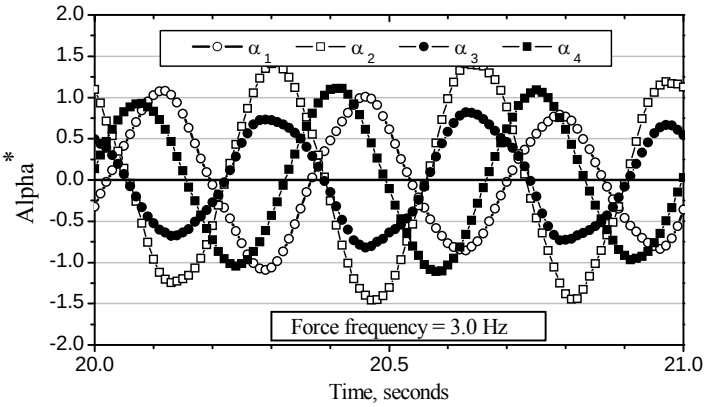

Figure 10. Time variations of normalized torsional moment α^* for a force frequency Ω = 3.0 Hz

The factor α^* varies with time and can be either positive or negative. For this particular case, it can be observed that peak values for all stories vary between -1.5 and 1.5, approximately.

Peak values of the amplification factor α^* computed during the steady-state response for each excitation frequency and building story are shown in Figure 11. For the 4th story a single value was not obtained because the phase angle was unknown because the exciter signal and the response were not synchronized. In the figure, this is suggested with vertical lines that indicate the range of values that the amplification factor would take. This range is the result of varying the phase angle of the exciting force with respect to the response, from null to full synchronization. It can be observed in this figure that peak values varied between 0.4 and 6.5, approximately. The largest values were found for Ω = 5.0 Hz, which was close to the sixth building modal frequency (building second torsion mode) computed with the calibrated finite element model of the building (De-la-Colina & Valdés 2007). The mean values of these peaks resulted to be as follows. Using the minimum peaks of 4th story: $\overline{\alpha^*}_{ssr1}$ = 1.82 while the standard deviation resulted to be σ_{ssr1} = 1.65 (coefficient of variation cov_{ssr1} = 0.9). On the other hand, using the maximum peaks of 4th story: $\overline{\alpha^*}_{ssr2}$ = 2.05 while the standard deviation resulted to be σ_{ssr2} = 1.73 (coefficient of variation cov_{ssr2} = 0.84).

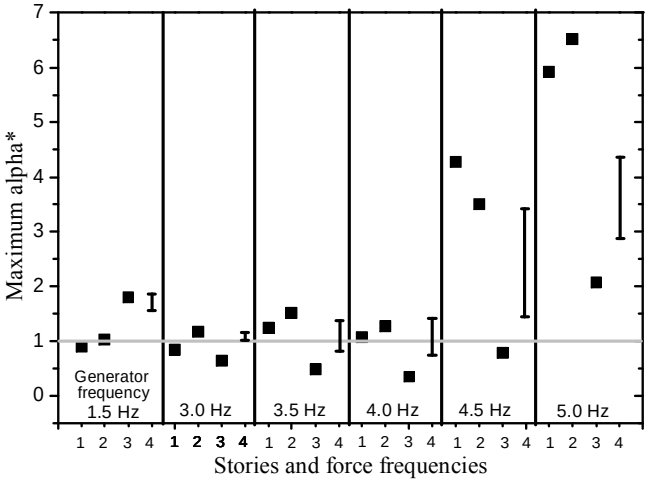

Figure 11. Peak values of α^* for the steady-state responses

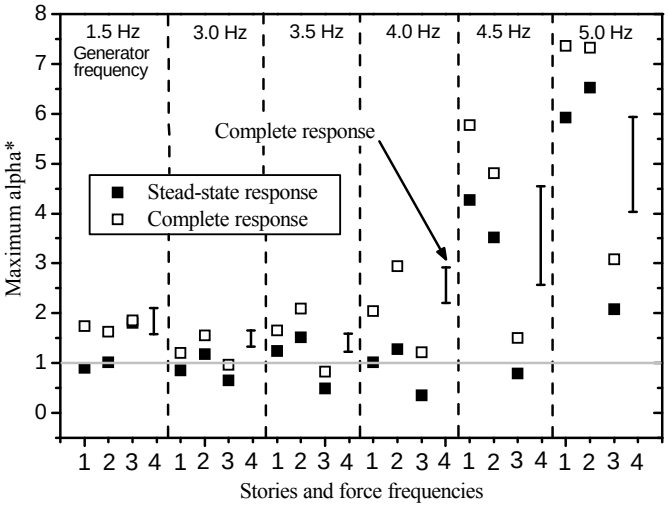

Figure 12. Peak values of α^* for both the steady-state and the whole responses.

When the complete response (transient and stationary) was considered, peak values resulted slightly larger than those computed for the steady-state response, as shown in Figure 12. Here the range vertical lines of 4th floor are shown only for the total response. Steady-state ranges are shown in Figure 11. In this case peak values varied between 0.8 and 7.3, approximately. For this total-response case, the mean values and the standard deviations resulted as follows. Using the minimum peaks of 4th story: $\overline{\alpha^*}_{tr1}$ = 2.59 while the standard deviation resulted to be σ_{tr1} = 1.89 (coefficient of variation cov_{tr1} = 0.73). On the other hand, using the maximum peaks of 4th story: $\overline{\alpha^*}_{tr2}$ = 2.84 while the standard deviation resulted to be σ_{tr2} = 1.99 (coefficient of variation cov_{tr2} = 0.70).

The results of the steady-state response are typical of a harmonic excitation which can be considered as representative of earthquakes recorded at soft soil. Therefore, steady-state results can be associated to soft-soil ground motions. On the other hand, whole-response results, which were governed by the transient response in all cases, correspond to an excitation that monotonically grows both in frequency and in magnitude up to the motor is steady. In this case, however, both exciter force magnitude and exciter frequencies do not recur. The beginning of this excitation could be similar to a short earthquake recorded in rock or firm soil. Due to the time variation of excitation frequencies, the authors believe that steady-state results are more realistic than results of the whole response.

It is clear from these results that story dynamic torsion moments can be significantly larger than the corresponding static moments. As anticipated, this is due to the effects of both rotational inertia (floor slab and story columns) and damping.

Supposing that α^* is comparable to α, some comparisons can be made between magnitudes of these factors. The mean values of the amplification factors for the steady-state response (for all stories and excitation frequencies) resulted for this case between 18% and 27% larger than the amplification factor α = 1.5 suggested by both the National Building Code of Canada (ACNBC 2005) and the Mexico City Building Code (DDF 2004). This percentage range results after considering the range of α values for the 4th story indicated before.

The application of an E-W force with an eccentricity e_s = 2.0 m on a representative analytical model of the building led to A_x = 1.436 (Equation 2). This value resulted between 21% and 30% smaller than the mean values of the amplification factors for the steady-state response (for all stories and excitation frequencies).

6 CONCLUSIONS

This paper presents estimations of experimentally obtained building dynamic torsion moments. These values were obtained from acceleration measurements taken from a four-story reinforced concrete building without accidental eccentricity subjected to forced vibrations. Excitation force was applied with one eccentric-mass force generator attached to the building roof. Forces were applied with an eccentricity of the exciter ($e_s \approx 0.1b$ and e_a= 0) and six frequencies (1.5, 3.0, 3.5, 4.0, 4.5, and 5.0 Hz). The procedure used to compute the dynamic torsion was based on the motion equations of a representative 12 degree-of-freedom model and the building recorded accelerations. The conclusions derived from this study are as follows.

The simple analysis presented in the introduction, which assumes that e_a is a static estimate of the ac-

cidental eccentricity, in dicates that within a s tatic analysis the amplification to account for dynamic effects should apply to both natural (inherent) and accidental eccentricities. Moreover, e_a should not be a dynamic estimation of the acciden tal eccentricity to avoid a double am plification if e_a is used with in a dynamic analysis.

Experimentally obtained results corroborate that building torsion response also depends on coupling between the excitation force frequency and the building mode frequencies associated with torsion (either pure torsion or tr anslation coupled with torsion). Current codes do not take into account explicitly this effect for static torsion design. In these experiments, test results showed that torsion m oments near resonance can be up to seven tim es larger than those without coupling.

The previous conclusions are considered the most relevant ones from this study, however other m inor conclusion are as follows. Peak values of the normalized torsional moment α^* computed during the steady-state response varied between 0.4 and 6.5, with mean values between $\overline{\alpha^*}_{ssr1}$ = 1.82 and $\overline{\alpha^*}_{ssr2}$ = 2.05 and standard deviations between σ_{ssr1} = 1.65 (cov_{ssr1} = 0.90) and σ_{ssr2} = 1.73 (cov_{ssr2} = 0.84). When the com plete response was considered, α^* varied between 0.8 and 7.3, with mean values between $\overline{\alpha^*}_{tr1}$ = 2.59 and $\overline{\alpha^*}_{tr2}$ = 2.84 and standard deviations between σ_{tr1} = 1.89 (cov_{tr1} = 0.73) and σ_{tr2} = 1.99 (cov_{tr2} = 0.70).

It is important to pinpoint that during these experiments the building remained in th e elastic range, so the (elastic) results rep orted here have a lim ited scope because during strong ground m otions the structures usually reach the inelastic behavior.

Results observed in this study are consistent with the analytical results obtained by Chandler et al. (1994), who also found that the response also depends on the m odel period. This dependency was found by studying ductility de mands in models with lateral-resisting elements along one direction only. It is important to pinpo int that Chandler et al. (1994) found this period dependency in term s of the lateral period of the m odel; on the other hand, the experimental results reported in this paper depend on the torsional frequencies of the building. Similar analytical results were reported by Correnza et al. (1995).

Results of other studie s (Kan & Chopra 1981) suggest that torsion effects decrease with inelastic deformation; therefore, it is exp ected that the amplification factors for buildings with in elastic response should be sm aller than t hose obtained from elastic responses.

REFERENCES

International Code Council, Inc. (ICC), 2006. *International Building Code (IBC)*. U. S. A.

Departamento del Distrito Federal (DDF), 2004. *Mexico City Building Code, complementary technical norms for earthquake design (MCBC).* México, D. F.

Associate Committee on the National Bu ilding Code (ACNBC), 2005. *National Building Code of Canada (NBCC)*. National Research Council of Canada. Canada.

Building Seismic Safety Cou ncil (BSSC), 2003. *NERPH Recommended provisions for seismic regulations for new buildings and other structures, 2003 Edition, Part 1: Provisions,* FEMA-450, Federal Emergency Management Agency, Washington D.C.

De la Llera , J. C. and C hopra, A. K., 1994. "Accidental and natural torsion in earthquake response and design of buildings", *Report No. UCB/EERC-94/07*, College of Engineering, University of California at Berkeley.

American Society of Civil Engineers (ASCE), 2005. *Minimum Design Loads for Buildings and Other Structures, ASCE-7-05*, American Society of Civil Engineers. Reston, VA.

Chandler, A., Correnza, J. C, and Hutchinson, G. L. 1994. "Period-dependent effects in seismic torsion response of code systems", *Journal of Structural Engineering, ASCE*, Vol. 120, No. 12, pp. 3418-3434.

Chandler, A. and Duan, X., 1993. "A modified static procedure for the design of torsionally unbalanced multistory frame buildings", *Earthquake Engineering and Structural Dynamics*, Vol. 22, No. 5, pp 447-462.

Chandler, A. and Hutchinson, G. L., 1988. "A modified approach to earthquake resistant design of torsionally coupled buildings", *Bulletin New Zealand National Society of Earthquake Engineering*, Vol. 21, pp 140-153.

Correnza, J. C., Hutchinson, G. L. and Chandler, A. M., 1995. "Seismic response of flexi ble-edge elements in code - designed torsionally unbalanced structures", *Engineering Structures*, Vol. 17, No. 3, pp. 158-166.

De-la-Colina, J., 2003. "Assessment of de sign recommendations for torsionally unbalanced multistory buildings", *Earthquake Spectra*, Vol. 19, No. 1, pp 47-66.

De-la-Colina, J., Acu ña, Q., Hernández, A. and Valdés, J., 2007. "Laboratory tests of steel simple torsionally unbalanced models", *Earthquake Engineering and Structural Dynamics*, Vol. 36, No. 7, pp 887-907.

Duan, X. N. and Chandler, A. N., 1993. "Inelastic seismic response of code-designed multistory frame buildings with regular asymmetry". *Earthquake Engineering and Structural Dynamics*, Vol. 22, No. 5, pp 431-445.

De-la-Colina, J. and Valdés, J., 2006. "Prueba s dinámicas de vibración forzada en un e dificio de c oncreto reforzado de cuatro niveles", *Memorias, XV Congreso Nacional de Ingeniería Estructural*, Puerto Vallarta, Jalisco, México (in spanish).

De-la-Colina, J. and Valdés, J., 2007. "Dynamic tests of a reinforced concrete building subjected to forced vibration", *Proceedings, 9th Canadian Conference on Earthquake Engineering*, Ottawa, Ontario, Canada, 1844-1853.

Kan, C. and Chopra, A., 1981. "Torsional coupling and earthquake response of simple elastic and i nelastic systems", *Journal of the Structural Division*, ASCE, Vol. 107, No. 8, pp 1569-1587.